Technical Memorandum No. 90

4853-11-T

ON THE SYNTHESIS OF DUAL-RESONANT CAVITIES WITH A DIGITAL COMPUTER

by

F. M. Waltz

Approved by: A. W. Naylor

A. W. Naylor

for

COOLEY ELECTRONICS LABORATORY

Department of Electrical Engineering
The University of Michigan
Ann Arbor

Task Order No. EDG-1
Contract No. DA-36-039 sc-89227
Signal Corps, Department of the Army
Department of the Army Project No. 3A99-06-001-01

December 1962

TABLE OF CONTENTS

LIST OF ILLUSTRATIONS

ABSTRACT

Mathematical analyses of multisection coaxial cavities (both in-line and re-entrant types) using a digital computer predict the possibility of shifting one of the spurious resonant frequencies (present in all coaxial cavities) to a desired frequency, thus allowing one cavity to do the work of two. "Fringing capacitance" at the conductor discontinuities is taken into account in the analysis by means of equations fitted to curves given in the references. The specific problem solved is the design of cavities to resonate a terminating capacitance (e.g., tube capacitance, "varactor" capacitance) at two harmonically-related frequencies, with the additional requirement that the two frequencies remain very nearly in the desired ratio despite wide variations (two-to-one or more) in the magnitude of the terminating capacitance. As one obvious application, a cavity meeting these requirements would make possible an inherently-aligned single-cavity frequency multiplier.

Computer flow charts and curves based on the computed results for specific cases are presented. Experimental cavities constructed according to the predicted designs have exhibited performance which is in very close agreement with the analysis, thus verifying both the validity of the method of analysis and the feasibility of the desired result.

Application of the same techniques to other and more general problems (e.g., single-cavity mixers, voltage-tunable filters) are suggested.

1. INTRODUCTION

In the UHF frequency range, coaxial cavities are widely used as resonant elements because they provide excellent performance and lend themselves to straightforward design, production, and tuning methods. Disadvantages include the spurious resonant modes frequently encountered, and the excessive size, weight, and complexity of the multiple-cavity circuits needed for all except the simplest applications. Thus, the paradoxical situation exists that coaxial cavities have extra (and usually unwanted) resonant frequencies, but that in a typical application a number of cavities must be used in order to obtain resonance at the desired set of frequencies.

This memorandum considers the use of multiple-section cavities to shift a spurious resonant mode to a desired frequency, so that one cavity can do the work of two. The specific problem considered in detail is the synthesis of cavities which resonate at two harmonically-related frequencies such that the resonant frequency ratio is insensitive to variations in the terminating capacitance (i. e., the desired frequency ratio is maintained within close limits in spite of wide variations in the terminating capacitance). Insensitivity to capacitance variation eliminates the need for selection or tuning of cavities to match individual tubes or allows the use of such cavities with time-varying capacitances.

A digital computer was used to obtain solutions to the system of simultaneous transcendental equations which result from the assumed mathematical model and the imposed conditions.

2. DISCUSSION

A uniform lossless coaxial cavity of length L and characteristic impedance Z_o, short-circuited at one end and with a capacitance C connected across the other end, resonates at an infinite number of frequencies f, each of which satisfies the following transcendental equation (neglecting end effects):

$$\frac{1}{2\pi fC} = Z_o \tan 2\pi f \frac{L}{c}, \tag{1}$$

where c is the velocity of propagation of electromagnetic radiation in the line under consideration. In general, these frequencies are not harmonically related.

In certain applications (e.g., frequency multipliers, mixers) it is desirable to have a single cavity resonate a terminating capacitance (e.g., tube capacitance, diode capacitance) at two harmonically-related frequencies. (Cavities having this property will be said to satisfy the dual-resonance condition.) A uniform section of coaxial line will not, in general, satisfy the dual-resonance condition.

It is shown below that coaxial cavities of the types depicted in Fig. 1 will produce the desired results. Consider first the in-line type [Fig. 1(a)], with lengths L_A and L_B, diameters d_1, d_2, and d_3, characteristic impedances[1] Z_A and Z_B, terminating capacitance C, and fringing capacitance C_F,[2] and assume that the conductors have infinite conductivity. This cavity configuration permits the independent choice of five parameters: d_1, d_2, d_3, L_A, and L_B. (C_F is not independent, but depends on the cavity dimensions [1,2].) Thus, it may be possible to satisfy as many as five independent design conditions. A few of

---

[1] Unless otherwise stated air dielectric is assumed.

[2] "Fringing capacitance" is a convenient device for representing the effect of the discontinuity in the center conductor. Whinnery, Jamieson, and Robbins have shown in Ref. 1 and Ref. 2 that the types of discontinuities considered in this memorandum can be accurately represented by one or more lumped frequency-independent capacitances, with the usual transmission-line equations applying to both sides of the capacitances. Further discussion of "fringing capacitances" and their effects is included elsewhere in this memorandum.

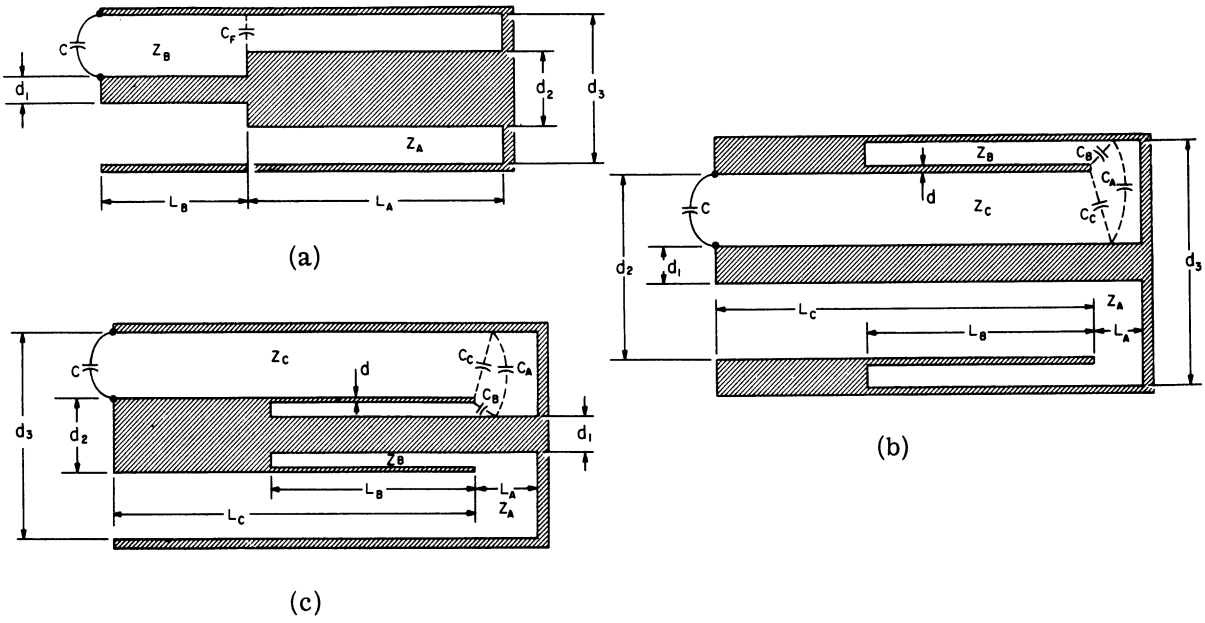

Fig. 1. Cavity configurations: (a) in-line; (b) external re-entrant; and (c) internal re-entrant.

the many conditions which might be of interest in particular applications are as follows:

a) Synthesize for a specified Z_A

b) Synthesize for a specified Z_B

c) Synthesize for specified diameters

d) Minimize overall cavity length, $L_A + L_B$

e) Synthesize so that the resonant frequencies shift as little as possible over a range of values of terminating capacitance.

f) Synthesize so that the n-to-one frequency relationship resulting from the satisfaction of the dual-resonance condition is maintained within close limits over a range of values of terminating capacitance, instead of only at one value of capacitance.

A cavity design which satisfied condition f) would be particularly desirable in applications where the terminating capacitance changes with time or where production or cost requirements preclude the tuning or matching of particular cavities to particular tubes. Attention is therefore directed toward cavity designs which satisfy the dual-resonance condition and condition f).

3. ANALYSIS OF IN-LINE CAVITY

Applying the transmission line equations to the section nearest the short circuit [see Fig. 1(a)], combining the resulting impedance with C_F, and applying the transmission line equations again, results in an expression for the cavity impedance Z(f), as seen from the open end, as follows:

$$Z(f) = jZ_B \frac{Z_A \tan\frac{2\pi}{c} fL_A + Z_B \tan\frac{2\pi}{c} fL_B - 2\pi f C_F Z_A Z_B \tan\frac{2\pi}{c} fL_A \tan\frac{2\pi}{c} fL_B}{Z_B - Z_A \tan\frac{2\pi}{c} fL_A \tan\frac{2\pi}{c} fL_B - 2\pi f C_F Z_A Z_B \tan\frac{2\pi}{c} fL_A} \tag{2}$$

The condition that C be resonated at frequency f by Z(f) is

$$j2\pi fC + \frac{1}{Z(f)} = 0 \tag{3}$$

Assume that there exists a pair of solutions to (3), $f = f_1(C)$ and $f = f_2(C)$. Ideally, f_2 should equal nf_1 for all values of C. This is not possible, in general, but can be approximated over a limited range of C near C_o if Z(f) is chosen so that

$$f_2(C_o) = n f_1(C_o) \tag{4}$$

and

$$\left.\frac{d f_2(C)}{dC}\right|_{C_o} = n \left.\frac{d f_1(C)}{dC}\right|_{C_o} . \tag{5}$$

These conditions will now be rewritten in a more usable form: Substitution of Eq. 3 into Eq. 4 yields

$$Z[f_1(C_o)] = n\, Z[f_2(C_o)] \tag{6}$$

as an equivalent to Eq. 4. Differentiating Eq. 3 with respect to C and solving for $\frac{df}{dC}$ yields

$$\frac{df}{dC} = \frac{-j2\pi f}{j2\pi C - \frac{\frac{\partial Z(f)}{\partial f}}{Z^2(f)}} \quad . \tag{7}$$

Substituting this into Eq. 5 and using Eqs. 4 and 6 allows Eq. 5 to be rewritten as

$$\left.\frac{\partial Z(f)}{\partial f}\right|_{f=f_1(C_o)} = n^2 \left.\frac{\partial Z(f)}{\partial f}\right|_{f=nf_1(C_o)} \quad . \tag{8}$$

Thus, the satisfaction of Eq. 3 at $f = f_1(C_o)$, and of Eqs. 6 and 8, is sufficient to guarantee that Z(f) satisfies both the dual-resonance condition and condition f) at $C = C_o$. Application of these equations to the impedance function given by Eq. 2 yields

$$X = \frac{\tan\theta_A + r\tan\theta_B - K\tan\theta_A\tan\theta_B}{r - \tan\theta_A\tan\theta_B - K\tan\theta_A} \tag{9}$$

(from Eq. 3)

$$\frac{\tan\theta_A + r\tan\theta_B - K\tan\theta_A\tan\theta_B}{r - \tan\theta_A\tan\theta_B - K\tan\theta_A} = n\,\frac{\tan n\theta_A + r\tan n\theta_B - Kn\tan n\theta_A\tan n\theta_B}{r - \tan n\theta_A\tan n\theta_B - Kn\tan n\theta_A} \tag{10}$$

(from Eq. 6)

$$\frac{r\theta_A + r^2\theta_B + (r\theta_A + \theta_B)\tan^2\theta_A + K\tan^2\theta_A(1 + \theta_B K) - 2r\theta_B K\tan\theta_A}{\cos^2\theta_B(r - \tan\theta_A\tan\theta_B - K\tan\theta_A)^2} =$$

$$n^2\,\frac{r\theta_A + r^2\theta_B + (r\theta_A + \theta_B)\tan^2 n\theta_A + K\tan^2 n\theta_A(1 + n^2\theta_B K) - 2rn\theta_B K\tan n\theta_A}{\cos^2 n\theta_B(r - \tan n\theta_A\tan n\theta_B - Kn\tan n\theta_A)^2} \tag{11}$$

(from Eq. 8)

where $X \triangleq \frac{1}{2\pi f_1 C_o Z_B}$, $r \triangleq \frac{Z_B}{Z_A}$, $\theta_A \triangleq \frac{2\pi}{c} f_1 L_A$,

$\theta_B \triangleq \frac{2\pi}{c} f_1 L_B$, and $K \triangleq 2\pi f_1 C_F Z_B$.

3. 1 Simplified Model, Neglecting Fringing Capacitance

The complexity of Eqs. 9, 10, and 11 prevents an easy determination of the ranges of the variables over which solutions are possible, if indeed any solutions exist at all. Most of the difficulty arises due to the complex inter-relationship of C_F and the cavity dimensions. Since in the applications contemplated in this memorandum C_F is usually not large compared to C, C_F will be neglected in the initial approach to the problem. Neglect of C_F implies that K = 0 in Eqs. 9, 10, and 11. Since X can be made to take on any positive value by proper choice of Z_B, the problem reduces to finding values of θ_A, θ_B, and r such that Eqs. 10 and 11 are simultaneously satisfied and such that the right-hand side of Eq. 9 is positive.

Solution of even this simplified problem in terms of known functions is for practical purposes not possible, but solution by numerical methods is not difficult. Figure 2 shows part of the solution to this problem in terms of the quantities r, X, θ_A, and θ_B for the case n = 2. Choice of a particular value for any one of the quantities, r, X, θ_A or θ_B immediately determines the other three. But since r and X depend on ratios of diameters, one degree of freedom still remains. That is, one of the three diameters can be chosen arbitrarily, after which the other two diameters can be determined from the definitions of r and X using the known values of f_1, C_o, r, and X, and the formulae

$$\frac{d_3}{d_2} = \log_e^{-1} \frac{Z_A}{60} \tag{12}$$

and

$$\frac{d_3}{d_1} = \log_e^{-1} \frac{Z_B}{60} \, . \tag{13}$$

3. 2 Effect of Fringing Capacitance

Analysis of the original model (hereafter referred to as the fringing capacitance model) is considerably more complicated than that of the simplified model. Also, because C_F depends on actual diameters, rather than ratios of diameters, solutions must be tabulated as a function of two parameters rather than only one, as was the case above. (See Fig. 2.)

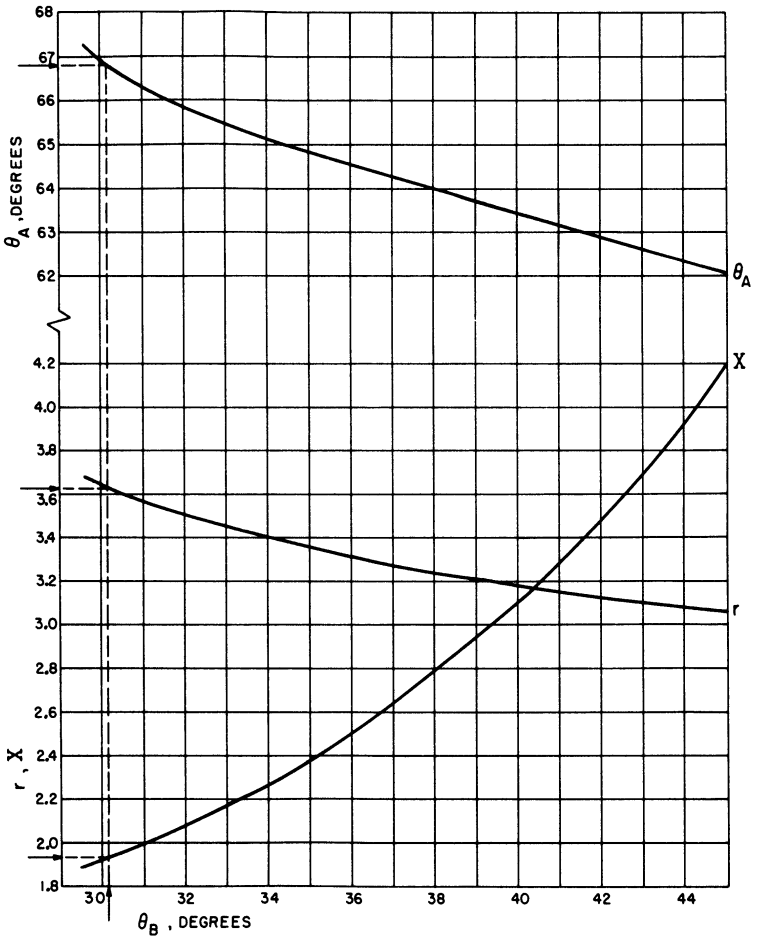

Fig. 2. Solutions for in-line cavity for n = 2, neglecting fringing capacitance.

To solve this problem, a digital computer was programmed [3] to find solutions to Eq. 10 for n = 2 for specified values of C_o, f_1, d_1, and d_3, and for a series of values of d_2. Figure 3 shows the flow chart for this computer program, from which it can be seen that, for each value of d_2, the computer finds the values of θ_A and θ_B (if they fall within the specified range) for which the desired capacitance is resonated at both the fundamental and the harmonic frequencies (i. e. , at which Eqs. 9 and 10 are satisfied). The computer also calculates and prints out the value of each side of Eq. 11 for each solution, thus allowing the cavity designer to pick (by interpolation) the one value of d_2 and the corresponding values of θ_A and θ_B which also satisfy Eq. 11.

[3] The computer determined the value of C_F in each case from equations which were fitted to the curves given in Refs. 1 and 2. If a particular application requires more accurate calculation of C_F than is possible by this method, then the complete procedure given in these references could be used.

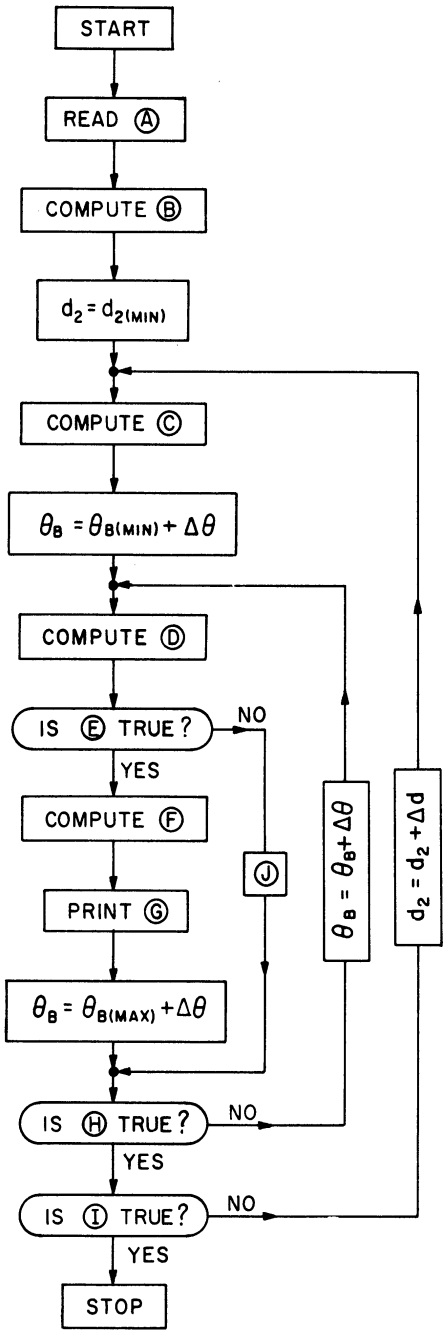

Fig. 3. Computer flow chart for in-line cavity computations.

DEFINITIONS and FUNCTIONS: (MKS units)

$X_F \triangleq$ Left side of Eq. 10, $\Delta X_F \triangleq$ Left side of Eq. 11

$X_H \triangleq$ Right side of Eq. 10, $\Delta X_H \triangleq$ Right side of Eq. 11

$F_1(\alpha,\tau) = \pi d_3 \times 10^{-10}(.334\,\alpha^2 - .410\,\alpha + .1372 + .00285\,\tau)$ (fitted to curves of [1,2])

$F_2(T_B) = r(X-T_B)/[T_B(X + K/X) + K + 1]$ (determines $T_A \triangleq \tan\theta_A$ so that $X_F = X$)

$$F_3(T_A,T_B) = 4\,\frac{T_A(1-T_B^2) + r\,T_B(1-T_A^2) - 4K\,T_AT_B/X}{r(1-T_A^2)(1-T_B^2) - 4T_A[T_B+K(1-T_AT_B)/X]}$$ {determines X_H, using Eq. 10 and trigonometric identities

$F_4(T_{B0},T_B,X_{H0},X_H) = [T_{B0}(X_H-X) + T_B(X-X_{H0})]\,(X_H-X_{H0})$ (interpolates to find value of T_B where $X_H = X$)

$F_5(\theta_{Ai},\theta_{Bi},T_{Ai},T_{Bi})$

$$= \frac{\theta_{Ai}\,rX^2(1+T_{Ai}^2) + \theta_{Bi}(r^2X^2 + T_{Ai}^2X^2 - 2rKX\,T_{Ai} + K^2T_{Ai}^2) + KX\,T_{Ai}^2}{\cos^2\theta_{Bi}\,[rX - T_{Ai}\,T_{Bi}\,X - K\,T_{Ai}]^2}$$ (from Eq. 11 & trig. identities)

$F_6(\theta_{Ai},\theta_{Bi},T_{Ai},T_{Bi})$

$$= 4(1+T_{Bi}^2)\,\frac{\theta_{Ai}\,rX^2(1+T_{Ai}^2)^2 + \theta_{Bi}[rX^2(1-T_{Ai}^2)^2 + 4\,T_{Ai}^2X^2 - 8\,rKX\,T_{Ai}(1-T_{Ai}^2) + 16K^2T_{Ai}^2] + 4KX\,T_{Ai}^2}{\left\{(1-T_{Bi}^2)[r(1-T_{Ai}^2)X - 4K\,T_{Ai}] - 4\,T_{Ai}\,T_{Bi}\,X\right\}^2}$$

(from Eq. 11 & trig. identities)

INSTRUCTIONS:

Ⓐ input data: f_1, C_0, d_1, $d_{2\min}$, Δd, $d_{2\max}$, d_3, $\theta_{B\min}$, $\Delta\theta$, $\theta_{B\max}$.

Ⓑ $\tau = d_3/d_1$; $Z_B = 60\log_e(d_3/d_1)$; $X = 1/(2\pi f_1 C_0 Z_B)$.

Ⓒ $\alpha = (d_3-d_2)/(d_3-d_1)$; $Z_A = 60\log_e(d_3/d_2)$; $r = Z_B/Z_A$; $C_F = F_1(\alpha,\tau)$.

$K = C_F/C_0$; $T_{B0} = \tan\theta_{B\min}$; $T_{A0} = F_2(T_{B0})$; $X_{H0} = F_3(T_{A0}, T_{B0})$.

Ⓓ $T_B = \tan\theta_B$; $T_A = F_2(T_B)$; $X_H = F_3(T_A,T_B)$.

Ⓔ $|X_{H0} + X_H - 2X| \leqq |X_{H0} - X_H|$ (curve intersection criterion)

Ⓕ $\theta_{A0} = \mathrm{Tan}^{-1}(T_{A0})$; $\theta_A = \mathrm{Tan}^{-1}(T_A)$; $T_{Bi} = F_4(T_{B0}, T_B, X_{H0}, X_H)$;

$T_{Ai} = F_2(T_{Bi})$; $X_{Hi} = F_3(T_{Ai}, T_{Bi})$; $\theta_{Ai} = \mathrm{Tan}^{-1}(T_{Ai})$; $\theta_{Bi} = \mathrm{Tan}^{-1}(T_{Bi})$

$L_A = 2.998 \times 10^8\,\theta_{Ai}/2\pi f_1$; $L_B = 2.998 \times 10^8\,\theta_{Bi}/2\pi f_1$;

$\Delta X_F = F_5(\theta_{Ai}, \theta_{Bi}, T_{Ai}, T_{Bi})$; $\Delta X_H = F_6(\theta_{Ai}, \theta_{Bi}, T_{Ai}, T_{Bi})$.

Ⓖ output data: θ_{A0}, θ_{Ai}, θ_A, L_A, θ_{B0}, θ_{Bi}, θ_B, L_B, Z_A, Z_B, r, C_F, d_2, X_{H0}, X_{Hi}, X_H, X, ΔX_F, ΔX_H.

Ⓗ $\theta_B \geqq \theta_{B\max}$

Ⓘ $d_2 \geqq d_{2\max}$

Ⓙ $X_{H0} = X_H$; $T_{B0} = T_B$, $T_{A0} = T_A$

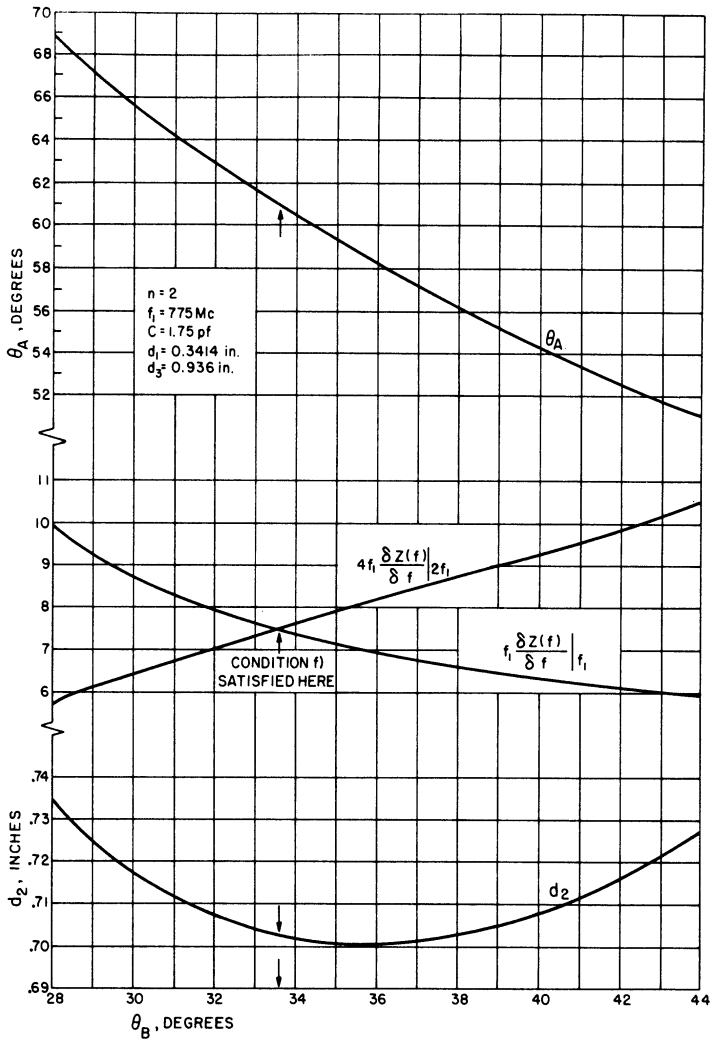

Fig. 4. Plot of typical computer output for in-line cavity, based on the fringing capacitance model.

The program was written in the MAD language, and included statements (not shown in Fig. 3) which provide for headings, output data format, overflow prevention, etc. Compilation of the program on an IBM 709 computer required 0.42 minute. Execution time varied with the ranges and increments of θ_B and d_2. A typical run, using 61 values of θ_B and 25 values of d_2, required 0.54 minute on the IBM 709. Figure 4 is a plot of the computer output for the particular case n = 2, f = 775 Mc, C = 1.75 pf, d_1 = 0.3414 inch, and d_3 = 0.936 inch. Arrows indicate the required values of θ_A, θ_B, and d_2.

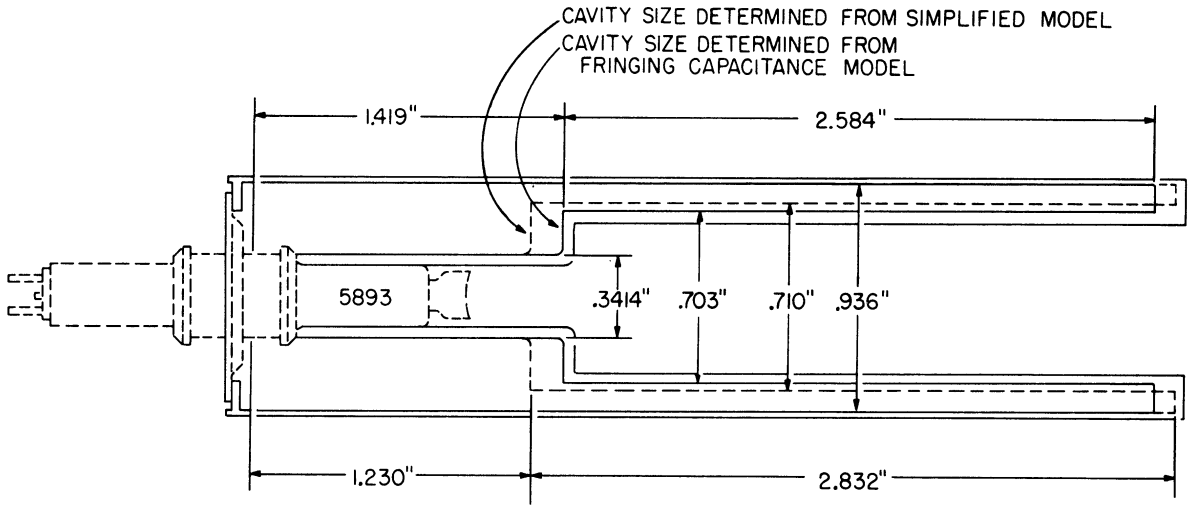

Fig. 5. Comparison of results from simplified model and fringing capacitance model.

To satisfy one (or two) conditions in addition to the dual-resonance condition and condition f), a series of solutions for various values of d_1 and d_3 could be obtained from which the desired solutions (or solution) could be selected.

3.3 Comparison of Results for Simplified Model with Results for Complete Model

To get some estimate of the error introduced by the neglect of fringing capacitance, a comparison was made for the particular case covered by Fig. 4. Figure 2 was used to determine the corresponding solution of the simplified problem for the same values of d_1 and d_3 (i.e., Z_B = 60.5136 ohms), and for C_o = 1.75 pf, and f_1 = 775 Mc (which result in X = 1.939). The arrows on Fig. 2 indicate the resultant values of θ_A, θ_B, and r. Figure 5 shows how the two results compare. The conclusion that can be drawn, in this case at least, is that, while the simplified model can be used to determine rather closely the ranges of d_2, θ_A, and θ_B over which solutions based on the fringing capacitance model can be expected, it is not sufficiently accurate to be used as a basis for actual cavity construction.

4. ANALYSES OF RE-ENTRANT CAVITIES

A major portion of the overall length of the cavity shown in Fig. 5 is taken up by the low-impedance section of coaxial line. Further study shows this to be generally true of the in-line type of cavity. The re-entrant designs shown in Fig. 1(b) and 1(c) make possible a considerable saving in both length and volume. Another advantage of the re-entrant designs is that, since these cavities have seven parameters (i.e., d_1, d_2, d_3, d, L_A, L_B, and L_C), it may be possible to satisfy seven design conditions, as opposed to the five conditions that were possible with the in-line type. The use of a dielectric other than air in the re-entrant section[4] adds an additional parameter to the system, bringing the total to eight.

The analyses of the re-entrant configurations are orders of magnitude more difficult than that of the in-line configuration, due to the additional parameters and also due to the fact that three fringing capactiances, C_A, C_B, and C_C, located as shown in Figs. 1(b) and 1(c), must be taken into account [1, 2].

The expression for Z(f) in this case is

$$Z(f) = jZ_C \frac{(A + B\tan\theta_A)(\cot\theta_C - 2\pi fC_CZ_C) - ABZ_C}{(A + B\tan\theta_A)(1 + 2\pi fC_CZ_C\cot\theta_C) + ABZ_C\cot\theta_C} \qquad (14)$$

where $A \triangleq (2\pi fC_AZ_A\tan\theta_A - 1)/Z_A$, $B \triangleq (2\pi fC_BZ_B - \cot\theta_B)/Z_B$, $\theta_A \triangleq \frac{2\pi}{c} fL_A$, $\theta_B \triangleq \frac{2\pi}{c} fL_B\sqrt{\epsilon_r}$, $\theta_c \triangleq \frac{2\pi}{c} fL_c$. Here ϵ_r is the relative dielectric constant of the material in the re-entrant line.

Digital computer programs were written to analyze both the external and the internal re-entrant configurations for the case n = 2. These programs differed only in the ex-

[4] If, as in the in-line case, the low-impedance section turned out to be longer than the high-impedance section, the internal re-entrant configuration could not be used in many cases, since the center conductor would not be long enough to accomodate the desired length of re-entrant line. A dielectric allows the effective length of the re-entrant line to be increased.

pressions used to calculate the characteristic impedances and the fringing capacitances. So that program complexity and computing time could be kept within bounds, the programs work with only four parameters: d_2, L_A, L_B, and L_c. The other parameters, d_1, d_3, d, and ϵ_r, as well as f_1, are constant for each set of computation.

Figure 6 shows the flow chart for this computer program. Here, for each value of d_2, L_B, and L_c, the computer seeks (in progressively smaller L_A-intervals, and then by interpolation) a value of L_A within the specified range which gives

$$C(f_1) = C(2f_1) \tag{15}$$

where C(f) is the capacitance resonated by the cavity at frequency f. [The function C(f) is obtained in this case by substituting Eq. 14 into Eq. 3 and solving for C.] If and when a value of L_A which causes Eq. 15 to be satisfied is found, the computer prints out L_A, L_B, L_c, d_2, and C. Also printed out are approximations to the reciprocals of the derivatives of Eq. 5, obtained as follows:

$$2\left.\frac{dC}{df}\right|_{f=2f_1} \approx \frac{2[C(2f_1) - C(1.998\,f_1)]}{2f_1 - 1.998\,f_1}; \quad \left.\frac{dC}{df}\right|_{f=f_1} \approx \frac{C(f_1) - C(.999f_1)}{f_1 - .999\,f_1} . \tag{16}$$

As before, it is left to the program user to determine (by a double interpolation) the values of d_2, L_A, L_B, and L_C at which Eq. 5 is satisfied, i.e., at which $2\left.\frac{dC}{df}\right|_{f=2f_1} = \left.\frac{dC}{df}\right|_{f=f_1}$. Fringing capacitances C_A, C_B, and C_C are computed from equations fitted to the curves of [1,2]. The specified values of L_A, L_B, L_C, and d_2 need not be equally spaced.

The program was written in the MAD language, and included statements (not shown in Fig. 6) which provided for headings, output data format, overflow prevention, etc. Compilation of the program on an IBM 7090 required 0.76 minute. Execution time varied with the number of values of L_A, L_B, L_c, and d_2 chosen. A typical run, using 31 values of L_A, 5 of L_B, 5 of L_c, and 6 of d_2, required 0.81 minute on the IBM 7090.

Figure 7 presents the results for the external re-entrant cavity for the special case n = 2, f_1 = 500 Mc, d_1 = .28125 inch, d_3 = 1.436 inches, d = .01 inch, and ϵ_r = 1.00. This figure can be applied to the design of particular cavities by choosing the capacitance that is to be resonated and a value for one other parameter (L_A, L_B, L_C, or d_2), and then

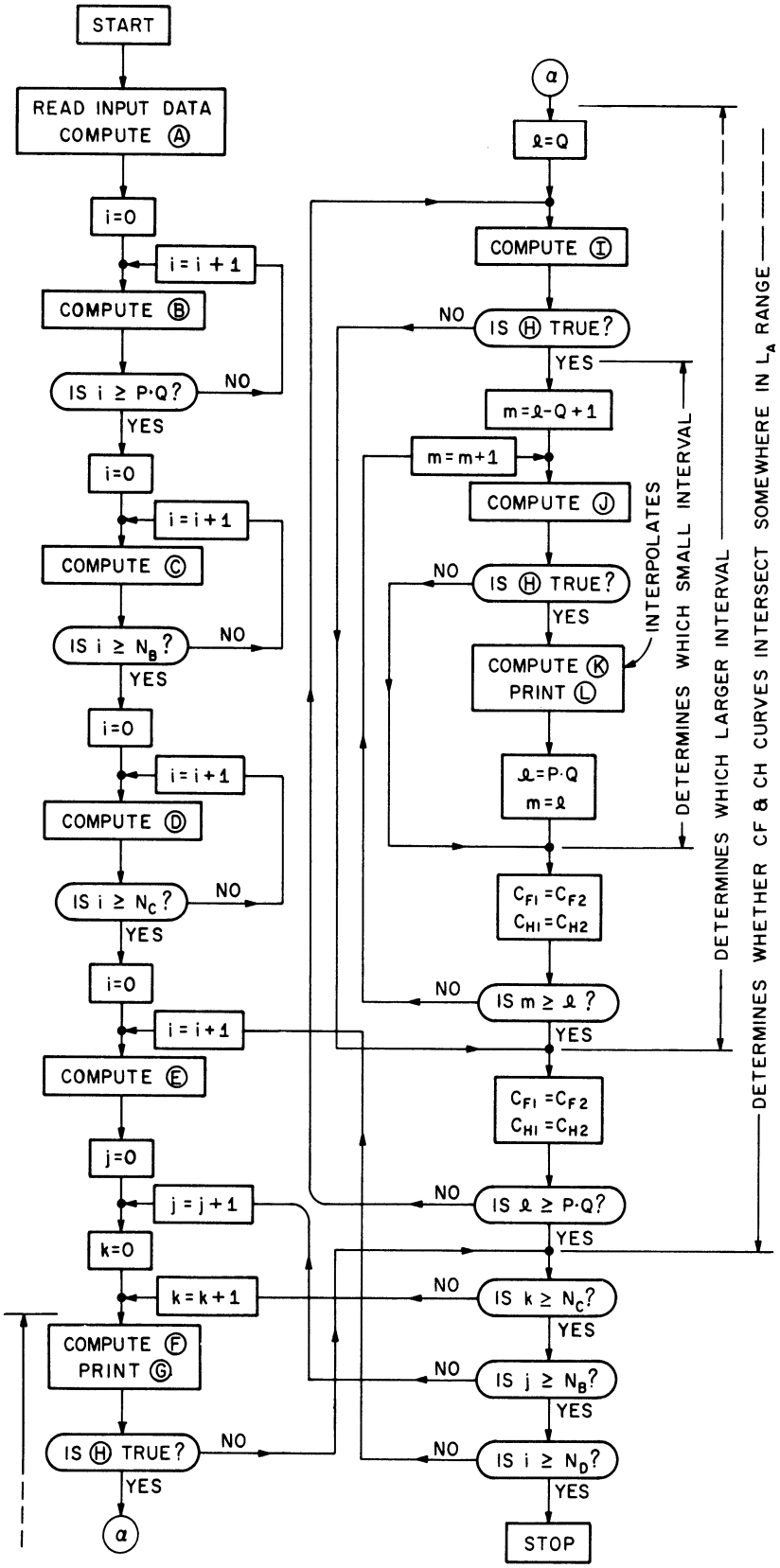

Fig. 6. Computer flow chart for external re-entrant cavity computations.

DEFINITIONS and FUNCTIONS: (MKS units)

C_F = capacitance resonated by cavity at fundamental frequency

C_H = capacitance resonated by cavity at harmonic frequency

PR = proximity factor for fringing capacitances

$F_1[\omega, T_A, CT_B, CT_C] = -\frac{Y_C}{\omega} \cdot \frac{(G_A + G_B T_A)(\omega C_C CT_C + Y_C) + CT_C G_A G_B}{(G_A + G_B T_A)(Y_C CT_C - \omega C_C) - G_A G_B}$, where

$G_A = \omega C_A T_A - Y_A$, and $G_B = \omega C_B - Y_B CT_B$.

INSTRUCTIONS: (parentheses indicate integer indices)

INPUT DATA: $f_1, \epsilon, d_1, d_3, d, P, Q, L_A(0), \ldots, L_A(P\cdot Q), N_B, L_B(0), \ldots, L_B(N_B)$,
$N_C, L_C(0), \ldots, L_C(N_C), N_D, d_2(0), \ldots, d_2(N_D)$

Ⓐ $\tau = d_3/d_1$, $K_1 = 2\pi f_1/2.998 \times 10^8$, $K_2 = 4\pi/(d_3 - d_1)$, $Y_A = 1/(60 \log_e \tau)$

$W = 2\pi f_1$, $X = 2W$, $Y = .999W$, $Z = 2Y$, $\Delta f = .001 f_1$, $E = \sqrt{\epsilon}$, $K_3 = K_1 E$,

$K_A = \pi(.375\tau^2 - 4.8629\tau + 16.213) \times 10^{-12}$, $A_A = -.050019\tau^2 + .590242\tau - .972512$,

$K_B = \pi(-.01278\tau^2 + .19363\tau - .19864) \times 10^{-12}$, $A_B = .57368\tau^2 + 7.83883\tau - 25.85208$

$K_C = \pi(.099911\tau^2 - 1.465289\tau + 7.990667) \times 10^{-12}$, $A_C = .00334\tau^2 - .05993\tau + .30615$

Ⓑ $T_{A1}(i) = \tan K_1 L_A(i)$; $T_{A2}(i) = 2T_{A1}(i)/[1 - T_{A1}^2(i)]$; $PR(i) = 1 + 2/(e^{K_2 L_A(i)} - 1)$

Ⓒ $CT_{B1}(i) = \cot K_3 L_B(i)$; $CT_{B2}(i) = \frac{1}{2}[CT_{B1}(i) - 1/CT_{B1}(i)]$; $CT_{B3}(i) = \cot .999 K_3 L_B(i)$;
$CT_{B4}(i) = \frac{1}{2}[CT_{B3}(i) - 1/CT_{B3}(i)]$

Ⓓ $CT_{C1}(i) = \cot K_1 L_C(i)$; $CT_{C2}(i) = \frac{1}{2}[CT_{C1}(i) - 1/CT_{C2}(i)]$
$CT_{C3}(i) = \cot .999 K_1 L_C(i)$; $CT_{C4}(i) = \frac{1}{2}[CT_{C3}(i) - 1/CT_{C3}(i)]$

Ⓔ $Y_B = E/[60 \log_e(d_3/(d_2(i) + 2d))]$; $Y_C = 1/[60 \log_e(d_2(i)/d_1)]$; $r = d_1/[d_2(i) + d]$
$C'_A = -d_3 K_A (A_A + r)(r - 1/\tau)(1 - r)/r^2$; $C'_C = d_3 K_C(r - 1/\tau)/(r - A_C)$;
$C'_B = d_3 K_B [-A_B + \tau/(r\tau - 1)][1.1881 - .008\tau - (18.81 - .8\tau)(r - .4)^2]$

Ⓕ $C_A = PR(0)C'_A$; $C_B = PR(0)C'_B$; $C_C = PR(0)C'_C$; $C_{F1} = F_1[W, T_{A1}(0), CT_{B1}(j), CT_{C1}(k)]$
$C_{H1} = F_1[X, T_{A2}(0), CT_{B2}(j), CT_{C2}(k)]$; $C_A = PR(P\cdot Q)C'_A$; $C_B = PR(P\cdot Q)C'_B$;
$C_C = PR(P\cdot Q)C'_C$
$C_{F2} = F_1[W, T_{A1}(P\cdot Q), CT_{B1}(j), CT_{C1}(k)]$; $C_{H2} = F_1(X, T_{A2}(P\cdot Q), CT_{B2}(j), CT_{C2}(k)]$.

Ⓖ PRINT $L_B(j), L_C(k), C_{F1}, C_{H1}, C_{F2}, C_{H2}, C'_A, C'_B, C'_C$

Ⓗ $|C_{F1} + C_{F2} - C_{H1} - C_{H2}| \leq |C_{F1} - C_{F2} - C_{H1} + C_{H2}|$ intersection criterion

Ⓘ $C_A = PR(\ell)C'_A$, $C_B = PR(\ell)C'_B$, $C_C = PR(\ell)C'_C$
$C_{F2} = F_1[W, T_{A1}(\ell), CT_{B1}(j), CT_{C1}(k)]$; $C_{H2} = F_1[X, T_{A2}(\ell), CT_{B2}(j), CT_{C2}(k)]$

Ⓙ $C_A = PR(m)C'_A$, $C_B = PR(m)C'_B$, $C_C = PR(m)C'_C$
$C_{F2} = F_1[W, T_{A1}(m), CT_{B1}(j), CT_{C1}(k)]$; $C_{H2} = F_1[X, T_{A2}(m), CT_{B2}(j), CT_{C2}(k)]$

Ⓚ $L'_A = L_A(m-1) + [L_A(m) - L_A(m-1)](C_{H1} - C_{F1})/(C_{F2} - C_{F1} - C_{H2} + C_{H1})$ (interpolation)
$T_{A5} = \tan K_1 L'_A$; $T_{A6} = 2T_{A5}/(1 - T_{A5}^2)$; $T_{A7} = \tan .999 K_1 L'_A$; $T_{A8} = 2T_{A7}/(1 - T_{A7}^2)$
$PR' = 1 + 2/(e^{K_2 L'_A} - 1)$, $C'_F = F_1[W, T_{A5}, CT_{B1}(j), CT_{C1}(k)]$
$C'_H = F_1[X, T_{A6}, CT_{B2}(j), CT_{C2}(k)]$, $C''_F = F_1[Y, T_{A7}, CT_{B3}(j), CT_{C3}(k)]$
$C''_H = F_1[Z, T_{A8}, CT_{B4}(j), CT_{C4}(k)]$; $\Delta C_F = (C'_F - C''_F)/\Delta f$; $\Delta C_H = (C'_H - C''_H)/\Delta f$

Ⓛ PRINT $L_A(m-1), L'_A, L_A(m), C_{F1}, C'_F, C_{F2}, C_{H1}, C'_H, C_{H2}, \Delta C_F, \Delta C_H$

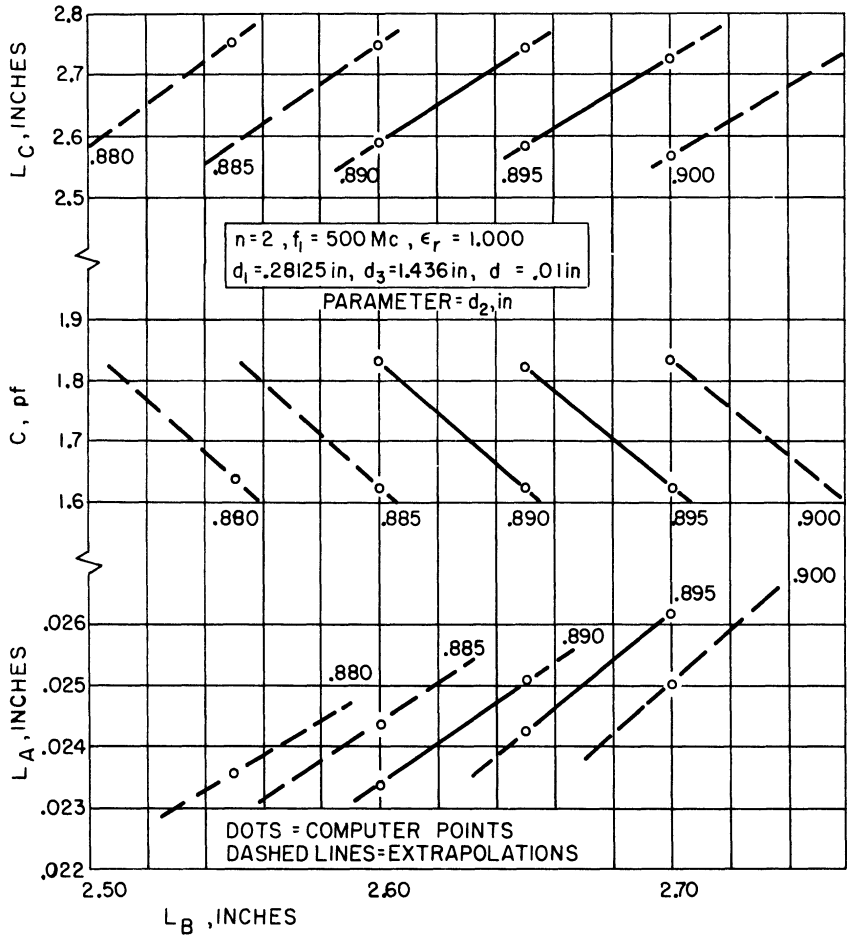

Fig. 7. Plot of typical computer results for the external re-entrant cavity model.

reading from the figure the values for the remaining parameters. As before, additional conditions could perhaps be satisfied by other choices of d_1, d_3, d, and ϵ_r.

The limited ranges of the parameters shown in this figure do not imply that no solutions exist outside of these ranges. However, in every special case that was investigated, the ranges were severely limited, (particularly the range of d_2). Usually one or more exploratory computer runs had to be made before the problem could be narrowed down to the ranges in which solutions were possible.

In this connection it should also be noted that all the examples considered in this memorandum involve standing-wave patterns analogous to a quarter-wave mode for the funda-

mental frequency and a three-quarter wave mode for the second harmonic. Other mode combinations are possible but were not considered here because minimum over-all length was desired.

The internal re-entrant model was investigated for the special case $n = 2$, $f_1 = 600$ Mc, $\epsilon_r = 2.10$ (Teflon), $d_1 = .28125$ in., $d_3 = .936$ in., and $d = .01$ in. Some solutions which satisfied both conditions were found, but all of them involved either small values of C or values of L_B larger than L_C (a physically-unrealizable configuration in most practical applications, as inspection of Fig. 1(c) will reveal). Trends observed in the computer output indicated that, in this case at least, a larger value of ϵ_r might yield more practical results. Further investigation of the internal re-entrant model was not carried out, however, because it was assumed that the validity of the approach and the approximations used could be adequately tested on the basis of results for the other two cavity types.

5. APPLICATION TO CAVITY DESIGN

Actual coaxial cavities typically depart from the models described above in two important respects:

a) some losses are present, and

b) the simple open-end construction shown in Fig. 1 is usually not used.

Losses are present due to the finite conductivity of the conductors, the external loading, and the shunt conductance of the terminating device (vacuum tube, "varactor," etc.). When these losses are reasonably small, however, they principally affect the Q of the cavity and have only minor effect on the resonant frequencies. Thus the models used here can be expected to give a reasonable approximation to the performance of well-designed and well-constructed cavities in many applications.

The conditions at the open end of actual cavities can also be fitted to the model, in many cases. A typical UHF vacuum tube, such as the one shown in Fig. 5, has anything but a constant conductor diameter inside the tube. Pencil triodes even have a re-entrant section inside the tube, since the grid is coaxial with the hollow plate conductor. It has been shown [1, 2], however, that if the cavity outside diameter is large compared to these internal conductor diameters of the tube, the fringing capacitances are small. Furthermore, the many individual fringing capacitances typically present (due to the many changes in diameter and dielectric constant in and near the tube) are typically located within a region the dimensions of which are small compared to a wavelength, so that they can often be well approximated by a single fringing capacitance at a properly chosen location.[5] Note also that, because of the satisfaction of condition f), the operation of the cavity will be insensitive to the small variation of the equivalent capacitance with frequency that does exist. Thus, it appears that the models considered here may be useful for the design of actual coaxial cavities.

---

[5] The equivalent capacitance can be determined with the methods of Refs. 1 and 2, or by direct experiment. Experiments performed with a 5893 pencil triode in a simple cavity (1" outer conductor, 5/16" inner conductor) gave a value of C which was constant within 5% over the range investigated, 600 to 1400 Mc. Corresponding results can be expected for other devices and frequencies, as long as the wavelength is not too short.

6. EXPERIMENTAL RESULTS

To test the validity of the previously mentioned analyses, experimental cavities were constructed and tested. The lengths of the cavities were made adjustable, so that dimensions near as well as at the design dimensions could be evaluated.

Figure 8 shows the experimental results for an in-line cavity with $d_1 = .3414$ in., $d_2 = .703$ in., and $d_3 = .936$ in., which is the case discussed in Section 3.2 and shown in Fig. 5 (solid lines). Figure 8(a) reveals that the desired result can indeed be achieved, and at dimensions very close to the calculated dimensions. The pairs of curves in Fig. 8(b) show the effects of variations in the length dimensions away from the optimum values. It is apparent from these curves that, for small variations at least, the low-frequency curves are less sensitive to dimensional changes than the high-frequency curves, and that changes in L_B are more critical than changes in L_A. The lowest pair of curves is included to show that dimensions which deviate significantly from the calculated values produce greatly inferior results, and hence that the obtaining of the desired behavior is indeed neither a coincidence nor an inherent property of all such cavities.

The experimental external re-entrant cavity model was built to conform as closely as was practical[6] to the special case covered by Fig. 7. Lengths L_A, L_B, and L_C [see Fig. 1(b)] were adjustable. In this case, because there are three variables and only two conditions to be satisfied, a family of calculated results, rather than a single result, is to be expected. Therefore, exploration of a region including part of the calculated family, rather than verification of a single calculated design, was undertaken.

[6] A .010-inch-thick copper sheet was rolled and soldered into a tube, which was used as the re-entrant wall. This construction technique resulted in some variation in diameter and in concentricity.

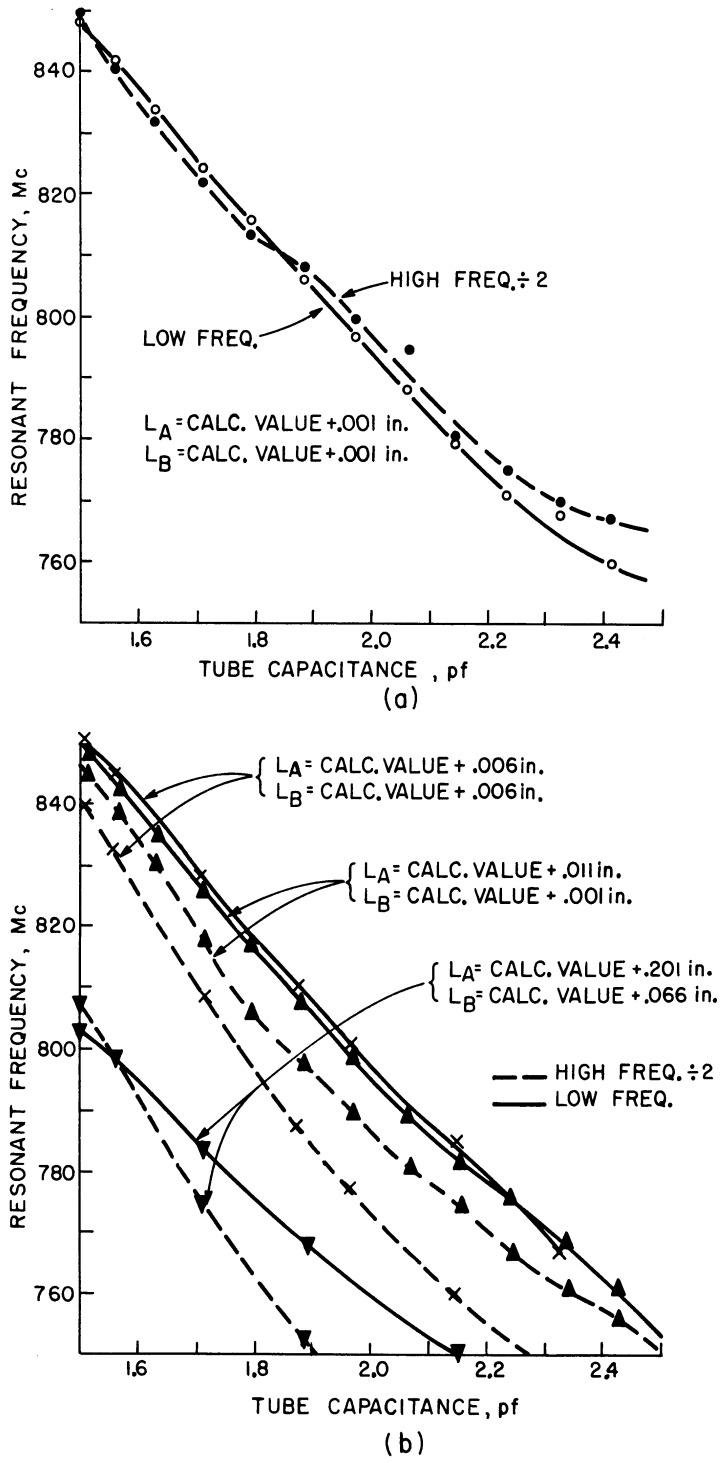

Fig. 8. Experimental results for in-line cavity. (a) Dimensions essentially equal to the calculated values. (b) Dimensions deviating from the calculated values.

Figure 9 shows some of the results obtained. Note that, while the separation between the curves in Fig. 9(a) is in general greater than that shown in Fig. 8(a) the curves in Fig. 9(a) remain close together over a wider range of capacitance variation. Limitations in the experimental equipment prevented checking the performance over an even wider capacitance range, but it appears from Fig. 9(a) that the curves should remain close to each other over a capacitance range considerably beyond two-to-one. Alternatively, some of the capacitance range could be sacrificed for the sake of better midrange performance, if the high-frequency curve could be shifted upwards slightly. There is good reason to believe that a set of values for L_A, L_B, and L_C near those used in obtaining Fig. 9(a) would accomplish this result. Figure 9(b) shows that here, as in the case of the in-line configuration, good performance is not a foregone conclusion.

In general, the experimental results for the re-entrant cavity did not agree with the calculated results as well as in the in-line case previously considered.[7] Nonetheless, the analyses for both configurations yielded results very close to those determined experimentally. For optimum performance in a given application, some tuning may be needed, but the analyses allow a drastic reduction in the range of the variables over which a solution must be sought. In the case of the re-entrant design, this is especially important, since an experimental cavity involving eight or nine manipulated variables (even if it could somehow be built) would be almost impossible to investigate experimentally in a reasonable length of time.

---

[7] This is believed to be due in part to the fact that the fringing capacitance approximations used become somewhat less accurate at the small values of L_A used, and in part to the limitations of the experimental setup, which rendered impractical an exact embodiment of the mathematical model and a full investigation of all combinations of L_A, L_B, and L_C which might have been of interest.

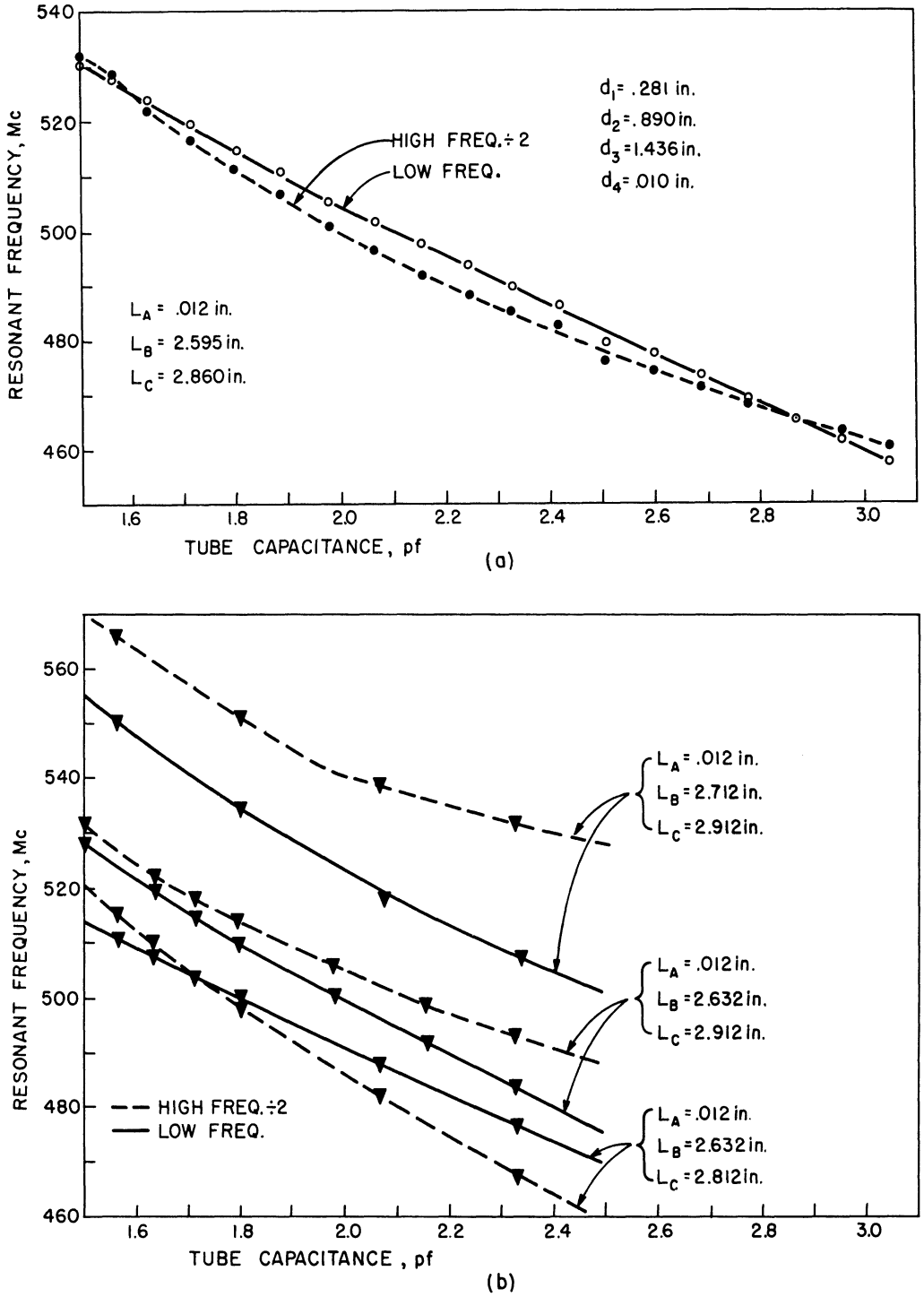

Fig. 9. Experimental results for external re-entrant cavity.

7. RELATED PROBLEMS

The results of this investigation, and the success of the mathematical model in dealing with this problem, suggest that the same techniques might be effective in the solution of different but related problems, some of which are as follows:

Synthesis of cavities which resonate at three or more frequencies which are in specified ratios, harmonically-related or not.

Synthesis of cavities which resonate at two or more frequencies which maintain constant frequency separations (as opposed to frequency ratios) over a range of terminating capacitances (i. e., for mixer applications).

Control of antiresonant frequencies in addition to or instead of resonant frequencies (i. e., for filter applications).

Synthesis of tuning or modulation devices of special characteristics, using voltage-variable capacitors to obtain capacitance variation.

8. CONCLUSIONS

This memorandum has primarily considered coaxial cavities which satisfy both the dual-resonance condition and the equal slope condition. The mathematical model which has been used predicts that the desired conditions can be met. Experimental cavities built according to computed results based on the mathematical model gave performance very close to the predicted performance, thus proving that the desired results are indeed obtainable, and demonstrating the usefulness of the method of analysis.

REFERENCES

1. J. R. Whinnery and H. W. Jamieson, "Equivalent Circuits for Discontinuities in Transmission Lines," Proc. IRE, Vol. 32, February 1944.

2. J. R. Whinnery, H. W. Jamieson, and T. E. Robbins, "Coaxial Line Discontinuities," Proc. IRE, Vol. 32, November 1944.

DISTRIBUTION LIST

Copy No.	
1-2	Commanding Officer, U. S. Army Electronics Research and Development Laboratory, Fort Monmouth, New Jersey, ATTN: Senior Scientist, Electronic Warfare Division
3	Commanding General, U. S. Army Electronic Proving Ground, Fort Huachuca, Arizona, ATTN: Director, Electronic Warfare Department
4	Chief, Research and Development Division, Office of the Chief Signal Officer, Department of the Army, Washington 25, D. C., ATTN: SIGEB
5	Commanding Officer, Signal Corps Electronic Research Unit, 9560th USASRU, P. O. Box 205, Mountain View, California
6	U. S. Atomic Energy Commission, 1901 Constitution Avenue, N. W., Washington 25, D. C., ATTN: Chief Librarian
7	Director, Central Intelligence Agency, 2430 E Street, N. W., Washington 25, D. C., ATTN: OCD
8	Signal Corps Liaison Officer, Lincoln Laboratory, Box 73, Lexington 73, Massachusetts, ATTN: Col. Clinton W. James
9-18	Commander, Armed Services Technical Information Agency, Arlington Hall Station, Arlington 12, Virginia
19	Commander, Air Research and Development Command, Andrews Air Force Base, Washington 25, D. C., ATTN: SCRC, Hq.
20	Directorate of Research and Development, USAF, Washington 25, D. C., ATTN: Electronic Division
21-22	Hqs., Aeronautical Systems Division, Air Force Command, Wright-Patterson Air Force Base, Ohio, ATTN: WWAD
23	Hqs., Aeronautical Systems Division, Air Force Command, Wright-Patterson Air Force Base, Ohio, ATTN: WCLGL-7
24	Hqs., Aeronautical Systems Division, Air Force Command, Wright-Patterson Air Force Base, Ohio - For retransmittal to - Packard Bell Electronics, P. O. Box 337, Newbury Park, California
25	Commander, Air Force Cambridge Research Center, L. G. Hanscom Field, Bedford, Massachusetts, ATTN: CROTLR-2
26-27	Commander, Rome Air Development Center, Griffiss Air Force Base, New York, ATTN: RCSSLD - For retransmittal to - Ohio State University Research Foundation

DISTRIBUTION LIST (Cont.)

Copy No.	
28	Commander, Air Proving Ground Center, ATTN: Adj/Technical Report Branch, Eglin Air Force Base, Florida
29	Chief, Bureau of Naval Weapons, Code RRR-E, Department of the Navy, Washington 25, D. C.
30	Chief of Naval Operations, EW Systems Branch, OP-35, Department of the Navy, Washington 25, D. C.
31	Chief, Bureau of Ships, Code 691C, Department of the Navy, Washington 25, D. C.
32	Chief, Bureau of Ships, Code 684, Department of the Navy, Washington 25, D. C.
33	Chief, Bureau of Naval Weapons, Code RAAV-33, Department of the Navy, Washington 25, D. C.
34	Commander, Naval Ordnance Test Station, Inyokern, China Lake, California, ATTN: Test Director - Code 30
35	Director, Naval Research Laboratory, Countermeasures Branch, Code 5430, Washington 25, D. C.
36	Director, Naval Research Laboratory, Washington 25, D. C., ATTN: Code 2021
37	Director, Air University Library, Maxwell Air Force Base, Alabama, ATTN: CR-4987
38	Commanding Officer - Director, U. S. Naval Electronic Laboratory, San Diego 52, California
39	Office of the Chief of Ordnance, Department of the Army, Washington 25, D. C., ATTN: ORDTU
40	Chief, West Coast Office, U. S. Army Electronics Research and Development Laboratory, Bldg. 6, 75 S. Grand Avenue, Pasadena 2, California
41	Commanding Officer, U. S. Naval Ordnance Laboratory, Silver Spring 19, Maryland
42-43	Chief, U. S. Army Security Agency, Arlington Hall Station, Arlington 12, Virginia, ATTN: IADEV
44	President, U. S. Army Defense Board, Headquarters, Fort Bliss, Texas
45	President, U. S. Army Airborne and Electronics Board, Fort Bragg, North Carolina
46	U. S. Army Anti-aircraft Artillery and Guided Missile School, Fort Bliss, Texas
47	Commander, USAF Security Service, San Antonio, Texas, ATTN: CLR
48	Chief, Naval Research, Department of the Navy, Washington 25, D. C., ATTN: Code 931
49	Commanding Officer, U. S. Army Security Agency, Operations Center, Fort Huachuca, Arizona

DISTRIBUTION LIST (Cont.)

Copy No.

50 President, U. S. Army Security Agency Board, Arlington Hall Station, Arlington 12, Virginia

51 Operations Research Office, Johns Hopkins University, 6935 Arlington Road, Bethesda 14, Maryland, ATTN: U. S. Army Liaison Officer

52 The Johns Hopkins University, Radiation Laboratory, 1315 St. Paul Street, Baltimore 2, Maryland, ATTN: Librarian

53 Stanford Electronics Laboratories, Stanford University, Stanford, California, ATTN: Applied Electronics Laboratory Document Library

54 HRB - Singer, Inc., Science Park, State College, Pennsylvania, ATTN: R. A. Evans, Manager, Technical Information Center

55 ITT Laboratories, 500 Washington Avenue, Nutley 10, New Jersey, ATTN: Mr. L. A. DeRosa, Div. R-15 Lab.

56 Director, USAF Project Rand, via Air Force Liaison Office, The Rand Corporation, 1700 Main Street, Santa Monica, California

57 Stanford Electronics Laboratories, Stanford University, Stanford, California, ATTN: Dr. R. C. Cumming

58 Stanford Research Institute, Manlo Park, California, ATTN: Dr. Cohn

59-60 Commanding Officer, U. S. Army Signal Missile Support Agency, White Sands Missile Range, New Mexico, ATTN: SIGWS-EW and SIGWS-FC

61 Commanding Officer, U. S. Naval Air Development Center, Johnsville, Pennsylvania, ATTN: Naval Air Development Center Library

62 Commanding Officer, U. S. Army Electronics Research and Development Laboratory, Fort Monmouth, New Jersey, ATTN: U. S. Marine Corps Liaison Office, Code AO-C

63 President, U. S. Army Signal Board, Fort Monmouth, New Jersey

64-72 Commanding Officer, U. S. Army Electronics Research and Development Laboratory, Fort Monmouth, New Jersey

ATTN: 1 Copy - Director of Research
1 Copy - Technical Documents Center ADT/E
1 Copy - Chief, Special Devices Branch, Electronic Warfare Div.
1 Copy - Chief, Advanced Techniques Branch, Electronic Warfare Div.
1 Copy - Chief, Jamming and Deception Branch, Electronic Warfare Div.
1 Copy - File Unit No. 2, Mail and Records, Electronic Warfare Div.
3 Cpys - Chief, Security Division (for retransmittal to BJSM)

73 Director, National Security Agency, Fort George G. Meade, Maryland, ATTN: TEC

DISTRIBUTION LIST (Cont.)

Copy No.

74 Dr. B. F. Barton, Director, Cooley Electronics Laboratory, The University of Michigan, Ann Arbor, Michigan

75-96 Cooley Electronics Laboratory Project File, The University of Michigan, Ann Arbor, Michigan

97 Project File, The University of Michigan Office of Research Administration, Ann Arbor, Michigan

98 Bureau of Naval Weapons Representative, Lockheed Missiles and Space Co., P. O. Box 504, Sunnyvale, California,
for forwarding to Lockheed Aircraft Corp.

99 U. S. Army Research Liaison Office, MIT, Lincoln Lab., Lexington 73, Mass.

100 Lockheed Aircraft Corp., Technical Information Center, 3251 Hanover Street, Palo Alto, California

Above distribution is effected by Electronic Warfare Division, Surveillance Department, USAELRDL, Evans Area, Belmar, New Jersey. For further information contact Mr. I. O. Myers, Sr. Scientist, Telephone 5961262.